Spatial and temporal evolution of Pine Island Glacier thinning, 1995–2006

D. J. Wingham,[1] D. W. Wallis,[1] and A. Shepherd[2,3]

Received 12 May 2009; revised 24 July 2009; accepted 5 August 2009; published 9 September 2009.

[1] We use ERS-2 and ENVISAT satellite radar altimetry to examine spatial and temporal changes in the rate of thinning of the Pine Island Glacier, West Antarctica, during the period 1995 to 2006. We show that the pattern of thinning has both accelerated and spread inland to encompass tributaries flowing into the central trunk of the glacier. Within the 5,400 km^2 central trunk, the average rate of volume loss quadrupled from 2.6 ± 0.3 km^3 yr^{-1} in 1995 to 10.1 ± 0.3 km^3 yr^{-1} in 2006. The region of lightly grounded ice at the glacier terminus is extending upstream, and the changes inland are consistent with the effects of a prolonged disturbance to the ice flow, such as the effects of ocean-driven melting. If the acceleration continues at its present rate, the main trunk of PIG will be afloat within some 100 years, six times sooner than anticipated. **Citation:** Wingham, D. J., D. W. Wallis, and A. Shepherd (2009), Spatial and temporal evolution of Pine Island Glacier thinning, 1995–2006, *Geophys. Res. Lett.*, *36*, L17501, doi:10.1029/2009GL039126.

1. Introduction

[2] The West Antarctic Ice Sheet (WAIS) contains sufficient water to raise eustatic sea level by over 3 metres [*Bamber et al.*, 2009], and has long been held susceptible to prolonged retreat resulting from small changes in climate or sea level [*Mercer*, 1978]. In consequence, the discovery [*Rignot*, 1998; *Shepherd et al.*, 2001] that the Pine Island Glacier (PIG), the largest of the WAIS ice streams, together with the Thwaites, Smith and Kohler glaciers further west [*Shepherd et al.*, 2002], is thinning due to ice dynamics, has commanded considerable attention.

[3] Although not confirmed by direct observation, the simultaneous thinning of the Amundsen Sea ice streams, and the lack of ice shelf thickening that might otherwise be expected as a result of an increased discharge of inland ice, make basal melting the likely source of the increased flow [*Shepherd et al.*, 2004]. The PIG is only lightly grounded for some 30 km upstream of its grounding line – the so-called 'ice plain' [*Corr et al.*, 2001]. Model studies showed that the longitudinal stress adjustment due to a reduction in ice shelf marginal drag [*Schmeltz et al.*, 2002] or basal stress in the ice plain [*Thomas et al.*, 2004b] may result in instantaneous thinning deep into the interior. A more detailed treatment [*Payne et al.*, 2004] indicated a more nuanced behaviour. Longitudinal stress adjustment was damped out within 80 km of the grounding line due to a high basal stress immediately upstream of the ice plane. Thinning farther upstream demanded a diffusive adjustment to the change in driving stress, a mechanism first suggested by *Joughin et al.* [2003] and supported by ground-based observations [*Scott et al.*, 2009]. This has the implication that changes presently occurring in the vicinity of the grounding line will result in ongoing thinning in the interior for decades to come.

[4] *Rignot* [2008] reports an increase of some 30 Gt yr^{-1} in the discharge of PIG between 1996 and 2007. We use contemporaneous ERS-2 and ENVISAT satellite altimetry to determine the source of this increased flux within the grounded ice. While the drawdown of the PIG is visibly more extensive in the ERS and ENVISAT altimeter surveys published since 2002 [*Rignot et al.*, 2008; *Wingham et al.*, 2006; *Zwally et al.*, 2005], this is not of itself evidence of increased thinning, since it may simply reflect the improved signal-to-noise ratio of longer time-series. The one study that has addressed changes in the rate of thinning (thinning rate) directly [*Thomas et al.*, 2004a], and reported the 2002–2004 thinning rate to be double that of 1992–1999, was limited to a single flight line and an interval of a single year.

2. Method and Results

[5] We use ERS-2 and ENVISAT radar altimeter observations to determine volume changes of the PIG during the period 1995 to 2008. Time-series of the change in surface elevation were developed at crossing points of the satellites ground tracks using the method of dual cycle cross-overs, described below. We used ERS-2 WAP data with Delft DE04 precise orbits, and ENVISAT GDR data with JPL GIM ionospheric corrections. Elevation measurements were corrected for the lag of the leading edge tracker, surface scattering variation [*Wingham et al.*, 2006], dry atmospheric mass, water vapour, the ionosphere, solid Earth tide, and ocean loading tide. At each crossing point and within each 35 day interval centred at time t there is one elevation, $a(t)$, measured on an ascending orbit and one, $d(t)$, on a descending orbit. We formed two time-series, one for each satellite, of elevation differences

$$\Delta h(t, t_0) = \frac{1}{2}((a(t) - d(t_0)) + (d(t) - a(t_0))) \qquad (1)$$

t_0 in either case denoting the first cycle. In the event a track was missing, the weight of ½ was set equal to 1. The time-series were averaged into bins of 10 km by 10 km. The

[1]Centre for Polar Observation and Modelling, Department of Earth Sciences, University College London, London, UK.
[2]Centre for Polar Observation and Modelling, School of Geosciences, University of Edinburgh, Edinburgh, UK.
[3]Now at School of Earth and Environment, University of Leeds, Leeds, UK.

Copyright 2009 by the American Geophysical Union.
0094-8276/09/2009GL039126

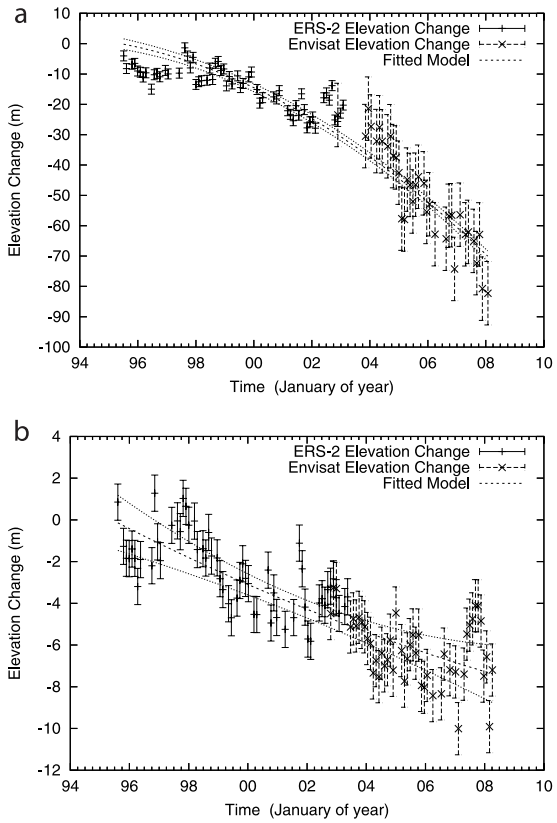

Figure 1. Time-series of elevation change 1995 to 2008 determined from ERS-2 and ENVISAT radar altimeters at the locations (a) A and (b) B shown in Figure 2, together with the best-fitting, accelerating thinning rate (dashed line) and its error (dotted lines). The increase in the error associated with the ENVISAT measurements arises because of the instrument cross-calibration.

errors in the time-series were estimated using the variance of the time-series formed on replacing the '+' in equation (1) with a '−', a procedure that removes the elevation change signal while retaining the error due to radar speckle that we expect to dominate the elevation change measurements at the spatial scale of the PIG basin [*Wingham et al.*, 2006].

[6] To cross-calibrate the satellites, the difference between the average elevation changes occurring during the overlap (October 2002 to May 2003) of the two missions was subtracted from the ENVISAT series to create single time-series of elevation change from the first cycle of ERS-2 in 1995. We did not use ERS-1 for this study because its frequent orbit-repeat changes complicate a comparison with the fixed-repeat ERS-2 and ENVISAT missions. In performing the cross-calibration, we found the dry atmospheric mass correction to the ERS-2 elevations to be in error, and so replaced it with a correction derived from NCEP surface pressures.

[7] On examining the time-series, we found many of them to have a curvature visible to the eye (e.g., Figure 1a). Rather than fitting a linear trend, as has been done previously, we fitted the time-series with the parabola

$$h(\tau) = h(0) + \dot{h}(0)\tau + \frac{1}{2}\ddot{h}(0)\tau^2 \tag{2}$$

where τ is the time measured from the mid-point of the observed interval. In consequence, the estimated thickening rate is the function of time

$$\dot{h}(\tau) = \dot{h}(0) + \ddot{h}(0)\tau \tag{3}$$

$\dot{h}(0)$ is the average thickening rate over the interval; $\ddot{h}(0)$ the average thickening acceleration.

[8] The parameters $h(0)$, $\dot{h}(0)$ and $\ddot{h}(0)$ were iteratively fit to each time-series using the least squares, Levenberg-Marquardt method. On each iteration, elevation changes departing further from the line than three-times the standard deviation of all departures were omitted. At the conclusion of this process, time-series as a whole were omitted if their standard deviation exceeded 1 m, or if the error arising in the cross-calibration exceeded 2 m, or if the time-series contained fewer than 6 points.

[9] To map the spatial pattern of the thinning rate at a location x, the rates at the cross-over bins, centered at x_i, were smoothed and interpolated using

$$\dot{h}_s(\tau, x) = \sum_{i=1}^{N} w_i(x)\dot{h}_i(\tau) \tag{4}$$

with Gaussian weights

$$w_i(x) = \frac{\exp\left(|x - x_i|^2/2r^2\right)}{\sum_{i=1}^{N} \exp\left(|x - x_i|^2/2r^2\right)} \tag{5}$$

where r = 50 km. Figure 2 shows the spatial pattern of the trend in 1995 and 2006; ice thinning rates increase rapidly towards the grounding line. To avoid biasing the smoothed thinning rate, we included in the summation of equation (4) the time-series (shown in Figure 1b) from the nearest location (point B in Figure 2) downstream of the grounding line, whose elevation rate we multiplied by 9.6 to account for its floatation [*Shepherd et al.*, 2004]. (We did not correct this series for the effects of ocean tides because the magnitude of the rate makes this unnecessary.)

[10] To estimate the rate of volume change, the smoothed thinning rate was integrated over three areas; the glacier trunk (as defined by *Shepherd et al.* [2001]), the glacier trunk and tributaries (bounded by the 100 m yr^{-1} velocity contour [*Joughin et al.*, 2003]), and the basin as a whole [*Shepherd et al.*, 2002]. The first two areas are shown in Figure 2. To estimate the error in the rates of volume change (volume rates), we used the parameter variances returned by the Levenberg-Marquardt fit and equation (3) to determine the error variance $\sigma_i^2(\tau)$ in the trend of each time-series (illustrated in Figure 1). Assuming the error to be series-to-series independent, the volume rate error variance arising from integrating over any particular *Area* is

$$\sigma_V^2(\tau) = \sum_i \sigma_i^2(\tau) \left(\int_{Area} dA\, w_i(x) \right)^2 \tag{6}$$

Table 1 gives values for the average volume rate and volume rate acceleration, and the volume rates for 1995 and

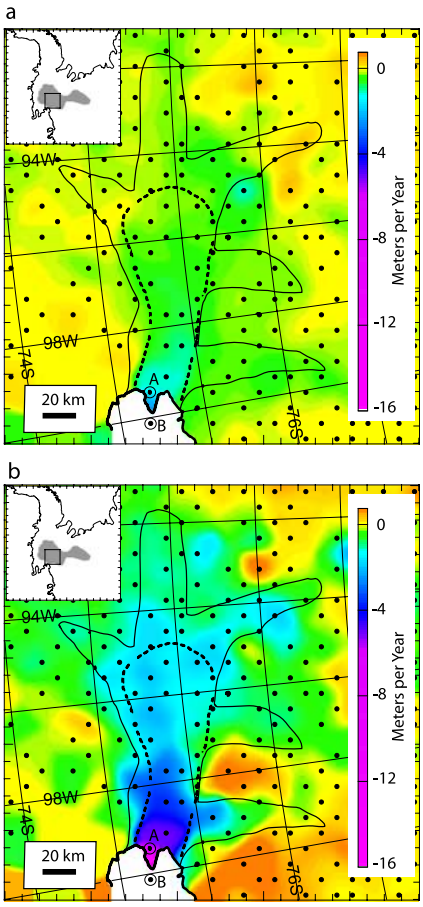

Figure 2. Thinning rate in the environs of the PIG in (a) 1995 and (b) 2006. The location of the time-series are shown by black dots; the time-series at the dots labelled 'A' and 'B' are shown in Figures 1a and 1b, respectively. Also shown are the boundaries of the glacier central trunk (dashed black line) and the glacier tributaries (black line)(see text for definitions), and the 1996 grounding line (thick black line).

2006, within the central trunk of the PIG and within the trunk and tributaries (see Figure 2). The figure of -2.6 ± 0.3 km^3 yr^{-1} for the 1995 glacier trunk thickening rate is greater (less negative) than that given previously [*Shepherd et al.*, 2001] due to our inclusion of additional time-series just upstream, and just downstream, of the grounding line.

3. Discussion

[11] We consider first the decadal average of the mass balance of the basin as a whole, which requires knowledge of the density associated with the volume rate. Within the glacier trunk and tributaries, the volume rate (Table 1) is far greater than expected fluctuations in snow accumulation, and must be associated with the drawdown of ice. In the slow-moving basin interior, however, the average elevation rate is considerably smaller, and the appropriate density depends on the contemporary average of the accumulation rate relative to the average over the centuries that determines the firn density structure [*Wingham*, 2000]. This is not known with useful accuracy, and, as has been done previously [*Wingham et al.*, 1998], we treat this uncertainty as an additional error whose magnitude is estimated from accumulation fluctuations observed in ice cores. We suppose the accumulation fluctuation to have a standard deviation of σ_m in mass and σ_ρ in density, and a temporal correlation duration of τ_c; the standard deviation of the average elevation rate fluctuation over an interval T will then be:

$$\sigma_h = \frac{1}{\rho_s}\left(\frac{\tau_c}{T}\right)^{\frac{1}{2}}\left(\sigma_m^2 + \left(\frac{\dot{m}_s}{\rho_s}\right)^2 \sigma_\rho^2\right)^{\frac{1}{2}} \quad (7)$$

where $\dot{m}_s$ is the mean accumulation rate and ρ_s the density of snow. Taking typical values of $\dot{m}_s$ = 400 kg m^{-2} yr^{-1}, σ_m = 120 kg m^{-2} yr^{-1} ice equivalent (i.e., 30% of the mean accumulation), τ_c = 1 year, ρ_s = 350 kg m^{-3}, σ_p = 30 kg m^{-3} (i.e., 10% of the mean) and T = 11 years, results in a thinning rate of 11 cm yr^{-1}, of which density fluctuations contribute some 2 cm yr^{-1}. This value is comparable only to the average elevation change observed in the PIG drainage basin interior (-0.11 ± 0.01 m yr^{-1}); changes in elevation within the tributaries and trunk are one to two orders of magnitude larger. The interior thickening is also part of a wider trend affecting neighbouring basins (e.g., the Antarctic Peninsula) where a dynamical argument is difficult to sustain. Assuming the interior fluctuations and the thinning of the tributaries and trunk have occurred at the densities of snow and ice, respectively, we estimate the changes in mass between 1995 and 2005 were -6.9 ± 0.6 Gt yr^{-1} within the trunk, -16.4 ± 1.1 Gt yr^{-1} within the tributaries and trunk, and -22.4 ± 11.3 Gt yr^{-1} within the basin as a whole. Our estimate of the basin-wide imbalance is comparable to the value of -24 ± 10 Gt yr^{-1} determined from SAR interferometry and a climate model [*Rignot*, 2008] in 2000, approximately the mid-point of the same decade; in one case the error reflecting uncertainty in accumulation fluctuation, in the other the uncertainty in accumulation mean.

[12] SAR interferometry shows also that the volume flux of ice across the PIG flexing line has increased progressively during the period of our survey [*Rignot*, 2008]. In 2006, the estimated rate of ice discharge was 30% (23 ± 5 km^3 yr^{-1}) greater than in 1996, an increase that has been equated to a change in the mass imbalance of the entire basin [*Rignot*, 2008]. However, our elevation data suggest that the rate of volume loss of the basin as a whole changed little over the same period: the increased drawdown of the fast-flowing ice appears to have been matched by acceler-

Table 1. Volume Changes of the Central Trunk and the Trunk and Tributaries of the Pine Island Glacier During the Period 1995 to 2006

Region	Area (km^2)	1995 Volume Rate (km^3 yr^{-1})	2006 Volume Rate (km^3 yr^{-1})	Decadal Average Volume Rate (km^3 yr^{-1})	Decadal Average Volume Acceleration (km^3 yr^{-2})
Trunk	5400	-2.60 ± 0.32	-10.09 ± 0.32	-7.49 ± 0.45	-0.65 ± 0.02
Trunk & tributaries	12800	-5.10 ± 0.51	-23.02 ± 0.51	-17.92 ± 0.72	-1.56 ± 0.04

ated growth in the basin interior. Because the accelerated growth occurs over slow-moving ice, it must result from a change in surface accumulation of snow (that is, the density associated with the change can be more securely identified than that of the average) – a conclusion that is supported by meteorological observations of enhanced snow accumulation during the same decade relative to the long-term mean [*Monaghan et al.*, 2006]. We deduce, therefore, that the rate of mass accumulation has increased by about 6 Gt yr^{-1}, leading to an estimated increase in mass loss through flow of 16 Gt yr^{-1} within the basin as a whole (a change that will be moderated to a degree by increased accumulation).

[13] We now consider changes in the fast flowing ice. Our data show that the observed increase in the 2002–04 thinning rate [*Thomas et al.*, 2004a] over that of 1992–96 [*Shepherd et al.*, 2002] reflects a continuous trend throughout the decade. In 1995 thinning was detectable only within the central trunk of the PIG, with rates in excess of 1 m yr^{-1} confined to the ice plain; by 2006, thinning encompassed all tributaries of the glacier, with rates exceeding 1 m yr^{-1} extending to 100 km upstream of the grounding line. At distances up to 50 km inland of the ice plain, the (instantaneous) thinning rates we obtain for 2003 are about half of those reported earlier for 2002–04 [*Thomas et al.*, 2004a], and we find no evidence of thinning further than 200 km from the grounding line. This may reflect a cross-calibration problem in the estimated 2002–04 thinning rate [*Thomas et al.*, 2004a], or inter-annual fluctuations in snow accumulation [*Monaghan et al.*, 2006]. However, there is qualitative agreement with the much-larger acceleration of the ice plain thinning rate [*Thomas et al.*, 2004a]: at the grounding line, thinning rates increased from 3 m yr^{-1} in 1995 to 10 m yr^{-1} in 2006.

[14] The cumulative effect of thinning at the PIG grounding line (Figure 1a) amounts to a change of some 80 m during the period 1995 to 2008 (we extended the time series of Figure 1 to 2008 to establish whether they continued to straddle the grounding line). The time-series in Figure 1b is, however, located within 10 km of the 1996 grounding line and within the region identified as an ice plain [*Corr et al.*, 2001]. Although estimates of the total thinning required to bring the ice plain to floatation [*Corr et al.*, 2001; *Thomas et al.*, 2004b] are somewhat lower than the thinning we have recorded, and satellite imagery observed in 2004 suggest that the grounding line may have retreated farther inland [*Rignot*, 2008], there is no evidence in Figure 1b of floatation (which would express itself through a reduction in thinning by a factor of 9.6). We attribute this to the presence of exceptionally thick ice in the region of the observations (towards the centre of the glacier) that is made apparent in, for example, the finger-like geometry of the hinge line [*Rignot*, 1998]. Basal resistance in the ice-plain must now be greatly reduced; one consequence could be further acceleration of ice flow as was suggested [*Thomas et al.*, 2004b] and has since been observed [*Rignot*, 2008].

[15] Our observations are sufficient to characterise the detailed manner in which the PIG mass perturbation has evolved. Within the glacier trunk, the volume loss has quadrupled from 2.6 ± 0.3 km^3 yr^{-1} in 1995 to 10.1 ± 0.3 km^3 yr^{-1} in 2006, similar to rates determined using ground-based observations [*Scott et al.*, 2009] The glacier terminus is however, not the region of greatest accelerated thinning - the peak rate has occurred at a distance ~50 km inland, suggesting that increased driving stresses are important to the inward propagation of the thinning [*Scott et al.*, 2009]. Rapid thinning is also more widespread (Figure 2) and, given the certainty and progression of the elevation trend, it is interesting to speculate on the implications of continued acceleration of ice thinning, a theoretical possibility [*Weertman*, 1974]. We estimate that, if the volume rate of the PIG central trunk continues to accelerate at a rate of -0.65 ± 0.02 km^3 yr^{-2} then, based upon its present geometry [*Vaughan et al.*, 2006], this region will become entirely afloat within about 100 years – six times sooner than was anticipated [*Shepherd et al.*, 2001] based on the thinning rate in the mid-nineties.

4. Conclusions

[16] Because thinning of the PIG is no longer restricted to its central trunk, projections of its contribution to 21st century sea level rise must now account for potential mass losses within its wider drainage basin. The rapidity with which the imbalance has propagated inland is, for example, considerably faster than rates derived from numerical simulations of the glacier response to a short-lived external forcing as considered by [*Payne et al.*, 2004], and there is no evidence in the elevation data (e.g., Figure 1a) of evolution towards a condition of steady state (as one might expect if the glacier were, for example, recovering from an episode of accelerated flow some decades earlier - such as that of the late 1970's [*Joughin et al.*, 2003]). Rather, the imbalance is consistent with projections of the glacier response to either a continued forcing (as considered by [*Thomas et al.*, 2004b], albeit with a diffusive upstream adjustment) or an abrupt event sufficient to trigger irreversible retreat [*Schoof*, 2007; *Weertman*, 1974], and supports observations of progressively accelerating ice discharge [*Rignot*, 2008].

[17] If we consider the implications of accelerated thinning within the wider region encompassing the glacier trunk and its tributaries, then a volume of ice equivalent to ~30 mm of eustatic sea level rise would be lost to the oceans within 130–140 years. However, what remains unclear is the extent to which the remainder of the PIG drainage basin – enough ice to raise global sea levels by more than a metre – will become drawn down. Although the origin of the imbalance lies almost certainly within the surrounding ocean [*Payne et al.*, 2004; *Shepherd et al.*, 2004], it may be associated with either long-term warming of the southern oceans [*Gille*, 2002] or decadal variability in ocean circulation [*Thoma et al.*, 2008]. In consequence, an improved estimate of the sea level contribution due to the Amundsen Sea sector of West Antarctica will require both a detailed understanding of the timescale over which the ocean forcing has evolved, and a careful consideration of the extent to which the remainder of the inland ice may be affected.

[18] **Acknowledgments.** Supported by the UK Natural Environment Research Council (F14/G6/95). NCEP Daily Global Analyses provided by NOAA/OAR/ESRL (http://www.cdc.noaa.gov/).

References

Bamber, J. L., R. E. M. Riva, B. L. A. Vermeersen, and A. M. LeBroq (2009), Reassessment of the potential sea-level rise from a collapse of the

West Antarctic Ice Sheet, *Science*, *324*, 901–903, doi:10.1126/science.1169335.

Corr, H. F. J., C. S. M. Doake, A. Jenkins, and D. G. Vaughan (2001), Investigations of an "ice plain" in the mouth of Pine Island Glacier, Antarctica, *J. Glaciol.*, *47*, 51–57, doi:10.3189/172756501781832395.

Gille, S. T. (2002), Warming of the Southern Ocean since the 1950s, *Science*, *295*, 1275–1277, doi:10.1126/science.1065863.

Joughin, I., E. Rignot, C. E. Rosanova, B. K. Lucchitta, and J. Bohlander (2003), Timing of recent accelerations of Pine Island Glacier, Antarctica, *Geophys. Res. Lett.*, *30*(13), 1706, doi:10.1029/2003GL017609.

Mercer, J. H. (1978), West Antarctic Ice sheet and CO_2 greenhouse effect: A threat of disaster, *Nature*, *271*, 321–325, doi:10.1038/271321a0.

Monaghan, A. J., et al. (2006), Insignificant change in Antarctic snowfall since the International Geophysical Year, *Science*, *313*, 827–831, doi:10.1126/science.1128243.

Payne, A. J., A. Vieli, A. P. Shepherd, D. J. Wingham, and E. Rignot (2004), Recent dramatic thinning of largest West Antarctic ice stream triggered by oceans, *Geophys. Res. Lett.*, *31*, L23401, doi:10.1029/2004GL021284.

Rignot, E. J. (1998), Fast recession of a West Antarctic glacier, *Science*, *281*, 549–551, doi:10.1126/science.281.5376.549.

Rignot, E. (2008), Changes in West Antarctic ice stream dynamics observed with ALOS PALSAR data, *Geophys. Res. Lett.*, *35*, L12505, doi:10.1029/2008GL033365.

Rignot, E., J. L. Bamber, M. R. van den Broeke, C. H. Davis, Y. Li, W. J. Van den Berg, and E. van Meijgaard (2008), Recent Antarctic ice mass loss from radar interferometry and regional climate modelling, *Nat. Geosci.*, *1*(1), 1–4, doi:10.1038/ngeo.2007.69.

Schmeltz, M., E. Rignot, T. K. Dupont, and D. R. MacAyeal (2002), Sensitivity of Pine Island Glacier, West Antarctica, to changes in ice-shelf and basal conditions: A model study, *J. Glaciol.*, *48*, 552–558, doi:10.3189/172756502781831061.

Schoof, C. (2007), Ice sheet grounding line dynamics: Steady states, stability, and hysteresis, *J. Geophys. Res.*, *112*, F03S28, doi:10.1029/2006JF000664.

Scott, J. B. T., G. H. Gudmundsson, A. M. Smith, R. G. Bingham, H. D. Pritchard, and D. G. Vaughan (2009), Increased rate of acceleration on Pine Island Glacier strongly coupled to changes in gravitational driving stress, *Cryosphere*, *3*, 125–131.

Shepherd, A., D. J. Wingham, J. A. D. Mansley, and H. F. J. Corr (2001), Inland thinning of Pine Island Glacier, West Antarctica, *Science*, *291*, 862–864, doi:10.1126/science.291.5505.862.

Shepherd, A., D. J. Wingham, and J. A. D. Mansley (2002), Inland thinning of the Amundsen Sea sector, West Antarctica, *Geophys. Res. Lett.*, *29*(10), 1364, doi:10.1029/2001GL014183.

Shepherd, A., D. Wingham, and E. Rignot (2004), Warm ocean is eroding West Antarctic Ice Sheet, *Geophys. Res. Lett.*, *31*, L23402, doi:10.1029/2004GL021106.

Thoma, M., A. Jenkins, D. Holland, and S. Jacobs (2008), Modelling Circumpolar Deep Water intrusions on the Amundsen Sea continental shelf, Antarctica, *Geophys. Res. Lett.*, *35*, L18602, doi:10.1029/2008GL034939.

Thomas, R., et al. (2004a), Accelerated sea-level rise from West Antarctica, *Science*, *306*, 255–258, doi:10.1126/science.1099650.

Thomas, R. H., E. Rignot, P. Kanagaratnam, W. Krabill, and G. Casassa (2004b), Force-perturbation analysis of Pine Island Glacier, Antarctica, suggests cause for recent acceleration, *Ann. Glaciol.*, *39*, 133–138, doi:10.3189/172756404781814429.

Vaughan, D. G., H. F. J. Corr, F. Ferraccioli, N. Frearson, A. O'Hare, D. Mach, J. W. Holt, D. D. Blankenship, D. L. Morse, and D. A. Young (2006), New boundary conditions for the West Antarctic Ice sheet: Subglacial topography beneath Pine Island Glacier, *Geophys. Res. Lett.*, *33*, L09501, doi:10.1029/2005GL025588.

Weertman, J. (1974), Stability of the junction of an ice sheet and an ice shelf, *J. Glaciol.*, *13*, 3–11.

Wingham, D. J. (2000), Small fluctuations in the density and thickness of a dry firn column, *J. Glaciol.*, *46*, 399–412, doi:10.3189/172756500781833089.

Wingham, D. J., A. Ridout, R. Scharroo, R. Arthern, and C. K. Shum (1998), Antarctic elevation change from 1992 to 1996, *Science*, *282*, 456–458, doi:10.1126/science.282.5388.456.

Wingham, D. J., A. Shepherd, A. Muir, and G. J. Marshall (2006), Mass balance of the Antarctic ice sheet, *Philos. Trans. R. Soc., Ser. A*, *364*, 1627–1635.

Zwally, H. J., M. B. Giovinetto, J. Li, H. G. Cornejo, M. A. Beckley, A. C. Brenner, J. L. Saba, and D. H. Yi (2005), Mass changes of the Greenland and Antarctic ice sheets and shelves and contributions to sea-level rise: 1992–2002, *J. Glaciol.*, *51*, 509–527, doi:10.3189/172756505781829007.

A. Shepherd, School of Earth and Environment, University of Leeds, Leeds LS2 9JT, UK.

D. W. Wallis and D. J. Wingham, Centre for Polar Observation and Modelling, Department of Earth Sciences, University College London, Gower Street, London WC1E 6BT, UK. (djw@cpom.ucl.ac.uk)